

# Log-normal distribution for correlators in lattice QCD?

Thomas DeGrand

*Department of Physics, University of Colorado, Boulder, CO 80309, USA*

## Abstract

Many hadronic correlators used in spectroscopy calculations in lattice QCD simulations appear to show a log-normal distribution at intermediate time separations.

arXiv:1204.4664v1 [hep-lat] 20 Apr 2012

Recently, while performing numerical simulations of unitary fermion gases, the authors of Refs. [1–7] discovered that spectroscopic correlation functions of operators separated by a Euclidean time  $t$ , call them generically  $C(t)$ , show a log-normal distribution. In a review article [1], they presented high statistics plots of the distribution of propagator values of a Lambda-Lambda dibaryon state[8], which also show a beautiful Gaussian structure for  $\log C(t)$ . The width of the Gaussian increases roughly linearly with  $t$ . I have been doing simulations of quenched baryon spectroscopy in larger- $N$   $SU(N)$  gauge field backgrounds, and I see the same thing, although with lower statistics: compare Fig. 1.

Unitary Fermi gases, Lambda-Lambda dibaryons, and large- $N$  baryons are rather exotic objects for lattice study, and the question naturally arises, how common are log-normal distributions in lattice spectroscopy? I believe that they are ubiquitous. I observe them in the following data sets:

- Meson and baryon spectroscopy, and string tension data from Wilson loops, in quenched  $SU(3)$ ,  $SU(5)$  and  $SU(7)$  simulations at a lattice spacing of about 0.1 fm
- $N_f = 2$  flavor dynamical simulations at a similar lattice spacing
- Quenched  $SU(3)$  simulations with the Wilson action at  $\beta = 5.9$  and 6.1 and overlap valence fermions
- Simulations in the weak coupling phase of  $SU(3)$  gauge theory with two flavors of sextet-representation fermions

This is a qualitative observation. I do not know why it occurs, how general it might be, nor what it is good for. In order not to make the paper too long, and to avoid being too redundant, I will only show pictures from quenched QCD.

Let's set some definitions. With the  $n$ th moment of a set of random variables  $x_i$  ( $i = 1$  to  $N$ ) as

$$\mu_n = \langle x^n \rangle, \quad (1)$$

the  $n$ th cumulant  $\kappa_n$  is defined recursively as

$$\kappa_n = \mu_n - \sum_{m=1}^{n-1} \binom{n-1}{m-1} \kappa_m \mu_{n-m}. \quad (2)$$

The objects of our attention are some set of expectation values of correlation functions of pairs of operators  $O$

$$C(t) = \sum_x O_l(x, t) O_m(0, 0) \quad (3)$$

generated in a Monte Carlo simulation, a set of random variables,  $C_i(t)$  for the  $i$ th measurement. Their falloff with  $t$  gives mass values.

If the operators are built of fermion propagators (such as for a meson or baryon propagator), lattice symmetries (charge conjugation plus  $\gamma_5$  Hermiticity) tell us that the real part of  $C(t)$  carries the signal. In an infinite ensemble the imaginary part of  $C(t)$  would average to zero. So I will only consider sets of real variables  $C_i(t)$ . The  $x$ 's will be the logarithms of  $C(t)$ . At small and intermediate  $t$  all the  $C(t)$ 's in any data set have the same sign (positive, by definition). At the largest times, some of the  $C(t)$ 's in some correlation functions can fluctuate negative. When I calculate the cumulants of  $\log C(t)$ , I will simply discard these

wrong-sign entries from my analysis, and when I show a result I will report the number of discarded configurations.

I consider mesonic and baryonic correlation functions, and Wilson loops. The correlators I show which involve quark propagators use clover fermions with links smeared using normalized hypercubic (nHYP) smearing [9, 10]. The clover coefficient is set to unity. Most of my spectroscopic sets use an extended source (typically, a Gaussian product state is used as the source of the fermion propagator) and point sinks, projected onto zero three momentum. Some data sets use zero-momentum Gaussian sinks as well. The first class of correlators is not variational. The size of the source has typically been tuned to produce flat plateaus in effective mass plots. These are completely standard data sets for lattice simulations, although the largest lattice volumes are small by today's standards,  $16^3 \times 48$  sites.

The other set of correlators I consider are Wilson loops, used to compute the heavy quark potential. These are real quantities and should all have the same sign. Fluctuations can drive them negative and I will treat this situation as I do for mesonic or baryonic correlators. The loops come from lattice configurations which were nHYP smeared and gauge fixed to axial gauge.

I observe that over a wide range in  $t$  the second cumulant  $\kappa_2$  is much greater than the higher ( $n > 2$ ) cumulants. If a distribution is Gaussian, its first and second cumulants (the mean and standard deviation) are the only non-vanishing ones, so this ordering of moments means that the distributions of  $C(t)$  are approximately log-normal. I also observe the same ordering of size of the  $m$ th moment of the correlator  $M_n$ , defined as a power of the original correlation function

$$M_n(t) = (C(t))^n. \quad (4)$$

Moments of a log-normally distributed variable are also log-normal. Finally, I observe, like Refs. [1–7], that the second cumulant of  $\log C(t)$ ,  $\kappa_2$ , increases roughly linearly with time  $t$ . Log-normal behavior is most prominent at short and intermediate distances, but these are distances where effective mass plots are roughly constant, where one would take masses to publish as results.

Let us look at some examples. I begin with a data set of 80  $16^3 \times 32$  quenched  $SU(3)$  lattices at  $\beta = 6.0175$ . Hadronic correlators from this data set, at one  $\kappa$  corresponding to an Axial Ward Identity (AWI) quark mass in lattice units of about  $am_q = 0.055$ , are shown in Fig. 2. The errors on the  $\kappa_n$ 's come from a jackknife. Observe that  $\kappa_2$  is much larger than the other  $\kappa_n$ 's and increases linearly with  $t$ .

Fig. 3 shows a set of cumulants from moments. The higher cumulants become quite noisy. The second moment of the square of the pseudoscalar propagator, the square of the delta propagator, and the cube of the delta propagator all increase with  $t$  and they either dominate the other moments or remain the only cumulant with statistically significant signal.

Fig. 4 shows plots of  $\kappa_n$  vs  $t$  for several Wilson loops of temporal extent  $t$  from this data set. Distances of  $t = 4 - 6$  are the range from which potentials may begin to be reliably extracted. Cumulants for the second and third moments of the  $(1, 1, 1)$  loop (panel (b) of Fig. 4) are shown in Fig. 5. Evidently, these Wilson loop expectation values are also log-normal distributed.

Log normal distributions present a contradiction with a well-known expectation of the noise in correlators, which goes back to Lepage[11]. The (over) simplified version of the explanation is that while the signal  $C_H(t)$  decays as  $\sim \exp(-m_H t)$ , the noise in the channel involves the exponential decay of the absolute square of the correlator

$$\sigma^2(t) \sim |C(t)|^2 = \langle 0 || O(t) |^2 | O(0) |^2 | 0 \rangle \sim \exp(-m_2 t) \quad (5)$$

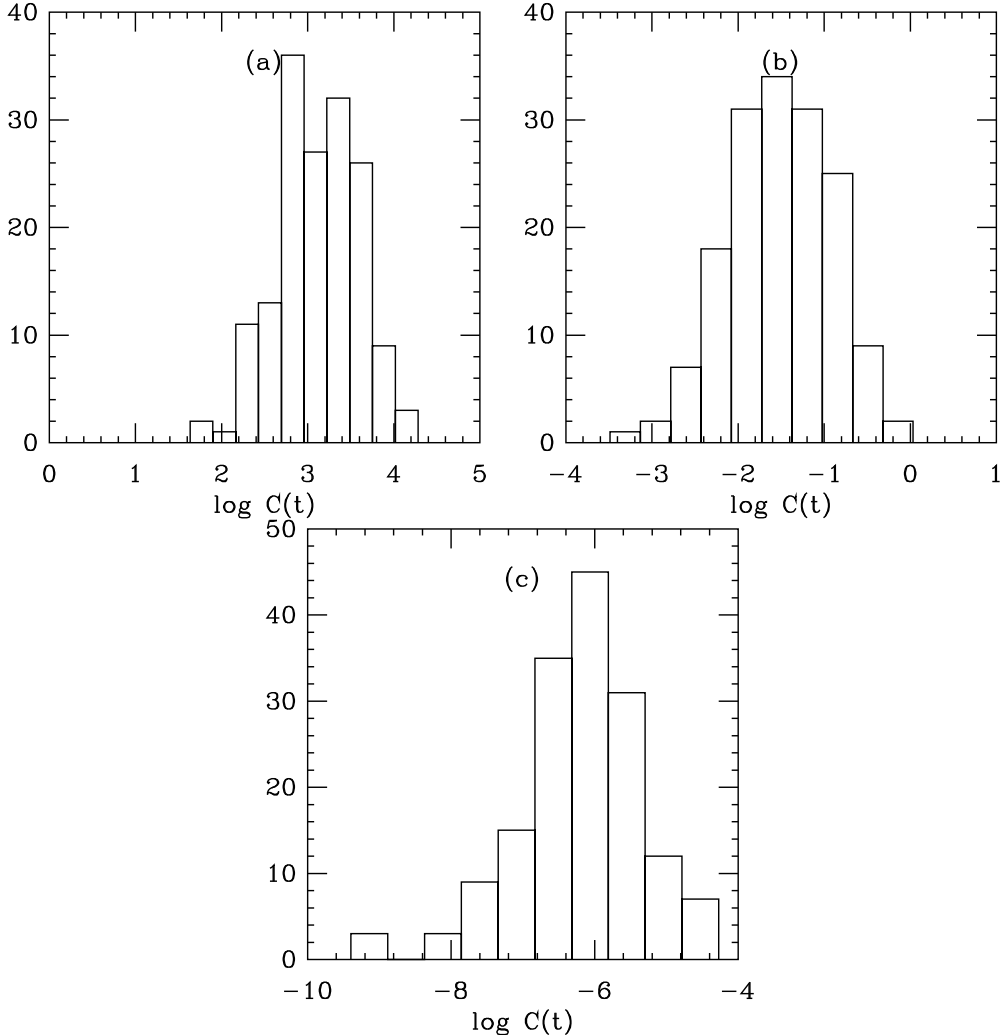


FIG. 1: Histogram of values of  $\log C(t)$  for the propagator of a  $J = 7/2$  baryon in  $SU(7)$ . Panels (a), (b), and (c) show results for  $t = 4, 6,$  and  $8$  respectively.

where  $m_2$  is the lightest state which can be created by the squared operator. For the pseudoscalar or the rho, the lightest state is the two-pseudoscalar state and  $\sigma(t)/C(t)$  should be roughly a constant for the pseudoscalar, roughly increasing exponentially as  $\exp((m_\rho - m_\pi)t)$  for the rho. (The energy of two particle states in a box includes an interaction term[12], which will reappear below.) For the ( $N$  color) baryon correlator, two different classes of behavior are expected for the moments[13]: when the moment number  $n$  is even, the correlator should couple to  $nN/2$  pseudoscalars and when  $n$  is odd, the lightest state will be a single baryon plus  $(n - 1)N/2$  pseudoscalars. Sometimes the squared correlator can couple to the vacuum, in which case  $\sigma^2(t)$  would be a constant. This is the situation for the scalar glueball mass or any Wilson loop.

Now consider the situation for a log-normal correlator. The average value of the  $n$ th moment is

$$\langle x^n \rangle = \exp(n\kappa_1 + \frac{n^2}{2}\kappa_2). \quad (6)$$

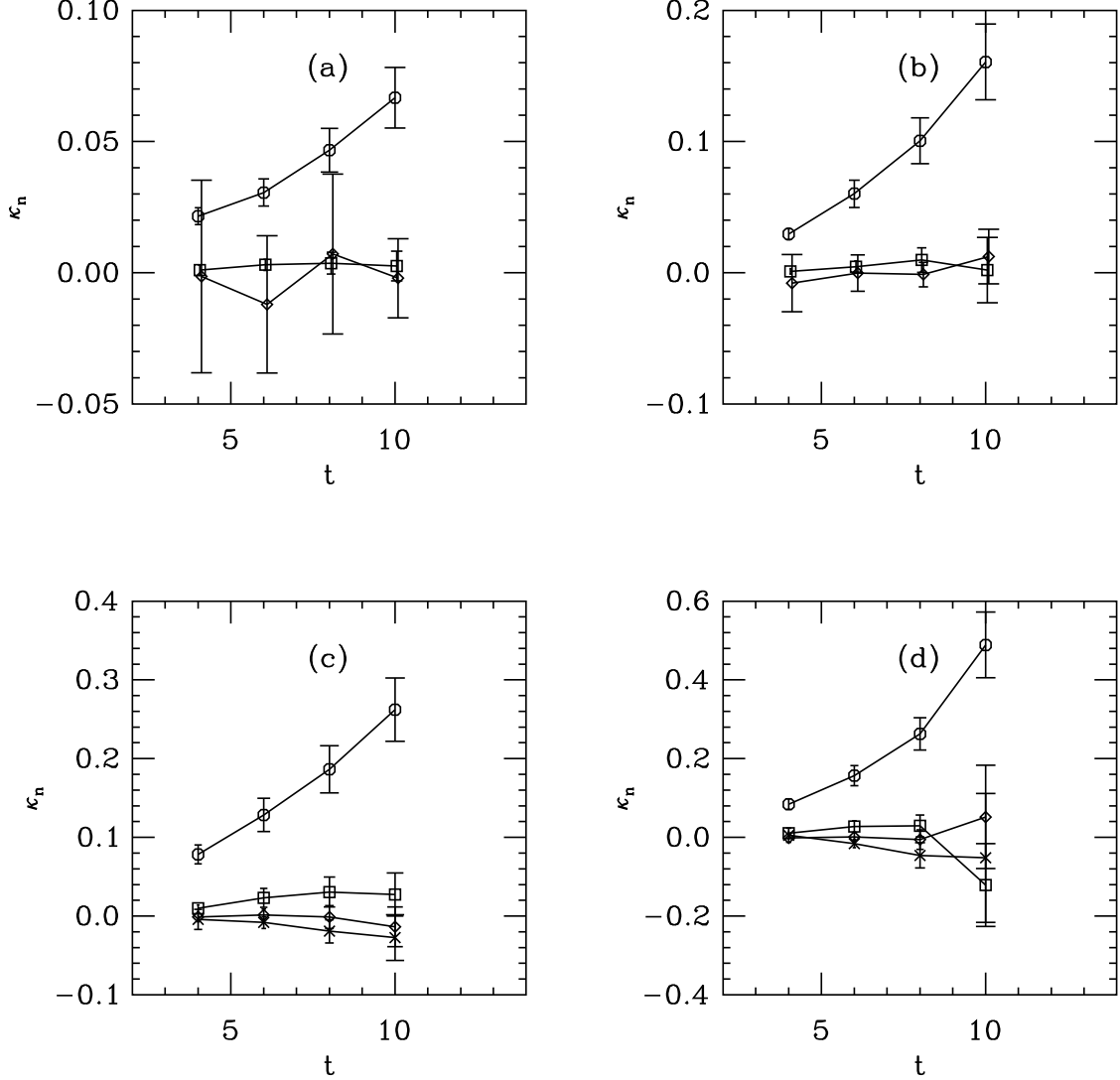


FIG. 2: Cumulants of  $\log C(t)$  for various smeared-to-point hadronic correlators of temporal extent  $t$ , from quenched  $SU(3)$  simulations at  $\beta = 6.0175$ ,  $\kappa = 0.125$ . (a) pseudoscalar, (b) vector, (c) proton (d) Delta. Labels are octagons for  $\kappa_2$ , squares for  $\kappa_3$ , diamonds for  $\kappa_4$ , crosses for  $\kappa_5$ . All correlators are positive at all  $t$  apart from one Delta correlator at  $t = 10$ .

The correlators  $C(t)$  decrease with  $t$  proportional to  $\exp(-Mt)$ . This says that both  $\kappa_1$  and  $\kappa_2$  should be linear functions of  $t$ , which is what we have seen. Call

$$\kappa_2(t) = tS + S_0. \quad (7)$$

We can define an effective mass from the logarithm of the ratio,

$$M = -\log \langle C(t+1) \rangle / \langle C(t) \rangle. \quad (8)$$

Eq. 6 tells us that the mass associated with the  $n$ th moment is

$$M_n = nM_1 - \frac{n(n-1)}{2}S \quad (9)$$

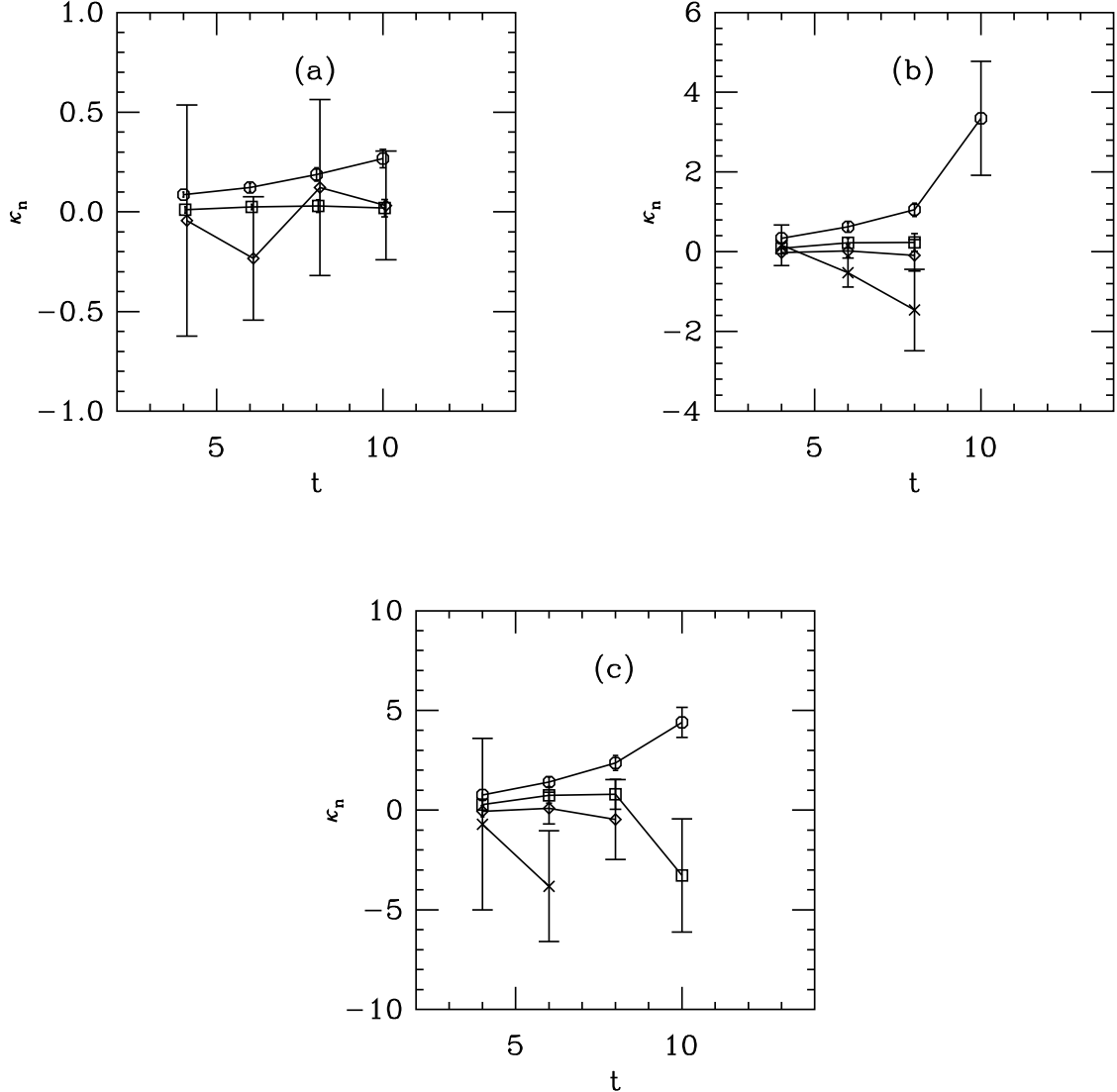


FIG. 3: Cumulants of  $\log M_n(t)$  for moments of various smeared-to-point hadronic correlators of temporal extent  $t$ , from quenched  $SU(3)$  simulations at  $\beta = 6.0175$ ,  $\kappa = 0.125$ . (a) square of the pseudoscalar correlator, (b) square of the Delta (c) cube of the Delta. Labels are octagons for  $\kappa_2$ , squares for  $\kappa_3$ , diamonds for  $\kappa_4$ , crosses for  $\kappa_5$  (baryons only; these are very noisy for the mesons).

that is, the log-normal distribution implies a pairwise interaction of the constituents of the  $n$ th moment. This is clearly inconsistent with Lepage-like behavior.

We can compare the two expectations for correlators. With the correlators in hand, just construct the correlation functions by averaging powers of the  $C(t)$ 's, the  $n$ th moments,  $M_n(t)$  and directly measure the effective mass of  $M_n(t)$ .

In Fig. 6, I compare the highest-spin baryon in  $SU(N)$ ,  $N = 3, 5, 7$ . The bare couplings have been tuned to match the lattice spacings. Panel (a) shows moments of the  $SU(3)$  delta. The lightest state is just the delta itself: its mass (in lattice units) is about 0.8. At its  $\kappa$  value the lattice pseudoscalar mass is 0.35, so the second moment (the octagons) should

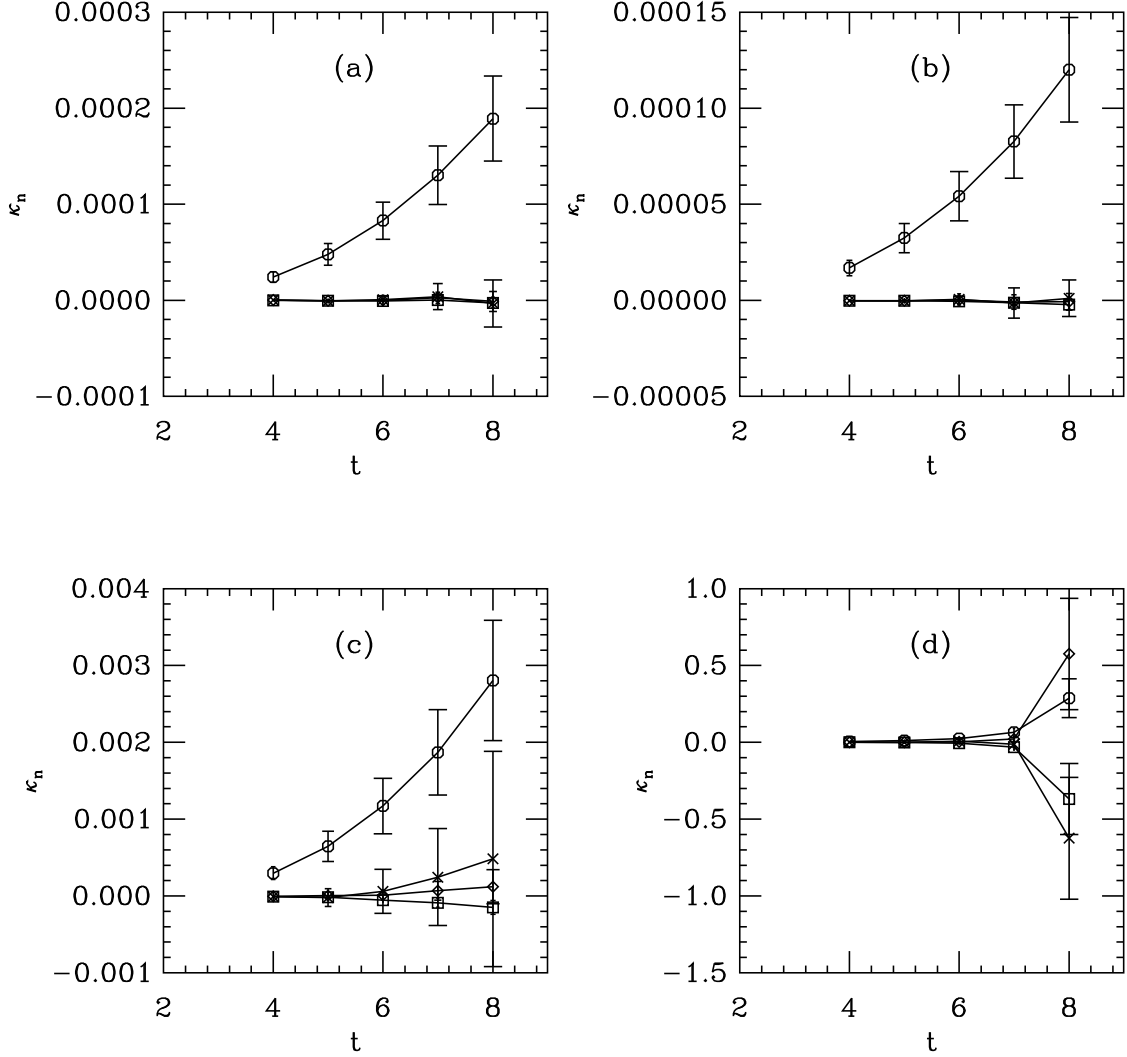


FIG. 4: Cumulants of  $\log C(t)$  for various Wilson loops of temporal extent  $t$ , from quenched  $SU(3)$  simulations at  $\beta = 6.0175$ . (a)  $r = 2$  planar loop; (b)  $\vec{r} = (1, 1, 1)$  loop; (c)  $r = 3\sqrt{2}$  loop; (d)  $r = 6\sqrt{2}$  loop. Labels are octagons for  $\kappa_2$ , squares for  $\kappa_3$ , diamonds for  $\kappa_4$ , crosses for  $\kappa_5$ . All correlators are positive at all  $t$ .

asymptote to a mass of  $3 \times 0.35 = 1.05$ . Instead, it sits at roughly twice the delta's mass. The second moment does not show a mass which is the sum of the delta mass plus three times the pseudoscalar, 1.85; it sits at roughly three times the delta mass.

For  $SU(5)$  (panel (b)), the situation is similar. Again the lattice pseudoscalar mass is 0.35. The baryon mass is about 1.5 in lattice units. The  $n$ th moment's effective mass is roughly just  $n$  times the baryon mass over a wide  $t$  range. At large  $t$  the masses tail over toward the Lepage formula. This is a soft statement, because the quality of the fit has deteriorated and it may be that the signal is just overwhelmed by noise, but it is certainly plausible. Note that this behavior occurs at much larger  $t$  than where the baryon's effective mass has gone to a plateau.

The situation for  $SU(7)$  (panel (c)) is again similar. (Here, the pseudoscalar mass is 0.4 in

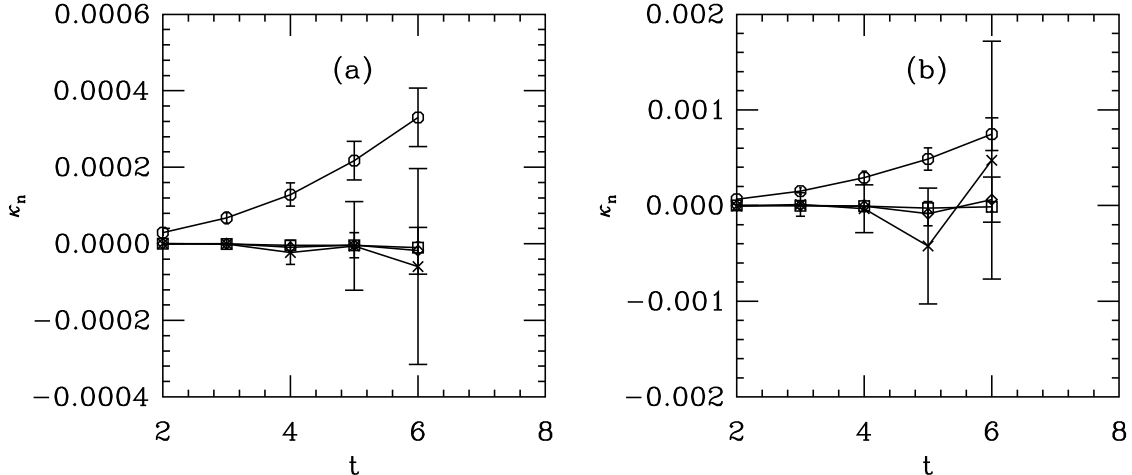


FIG. 5: Cumulants of  $\log M_n(t)$  from quenched  $SU(3)$  simulations at  $\beta = 6.0175$ . for the (a) second and (b) third moments of the  $r = (1, 1, 1)$  Wilson loop. Labels are octagons for  $\kappa_2$ , squares for  $\kappa_3$ , diamonds for  $\kappa_4$ , crosses for  $\kappa_5$ .

lattice units). Apparently Eq. 5 is only an asymptotic result. This is no surprise: the simple story was too simple. The correlator couples to everything with its quantum numbers, not just the lightest state:

$$M_n(t) = \sum_j Z_j \exp(-m_j t) \quad (10)$$

where  $m_j$  can include the  $n$ - baryon state. Presumably this is a dominant state, since some attempt was made to optimize the operators to produce a single baryon state in  $C(t)$ . So the asymptotic form may appear only at very late time.

Let's next test Eq. 9. I just take effective masses and, under a jackknife, compute  $\Delta M = nM - M_n$ . This should be linear in  $n(n+1)$ , and the slope should be given by the part of  $\kappa_2$  for  $\log C(t)$  which is linear in  $t$ . Fig. 7 shows this behavior quite nicely for hadron correlators in  $SU(3)$ . The line is a fit to  $S$  (see Eq. 9) over the range  $3 \leq t \leq 8$ .

Recall panel (b) of Fig. 6, showing the evolution of mass parameters at large  $t$ . Fig. 8 shows cumulants and the mass splitting for our  $SU(5)$   $J = 5/2$  state. Log-normal behavior works well at shorter  $t$  and fails at the largest  $t$ .

Finally, we return to potentials. Figs. 4, 9 and 10 show the consistency of log-normal behavior (dominant  $\kappa_2$ , effective masses scaling as in Eq. 9) at short distances, and when the effective mass for the moments falls, dominance of  $\kappa_2$  goes away.

So to summarize: At small and intermediate  $t$ , hadronic correlators show log-normal behavior. This is the  $t$  range where the Lepage formula does not describe the effective mass of the moments of  $C(t)$ . At large  $t$ , the Lepage formula does appear to describe the effective mass of the moments and correlators cease to be log-normal.

As a last observation, we can ask about volume dependence. I have two volumes for some of my quenched data sets. Figs. 11-12 show that the  $S$  parameter, the slope of  $\kappa_2$  with  $t$ , often scales inversely with the simulation volume. I do not have enough other data sets to say more about this.

Are there any consequences of this observation? I can think of two.

First, the authors of Refs. [1-7] have shown that, for their data sets, noisy signals can



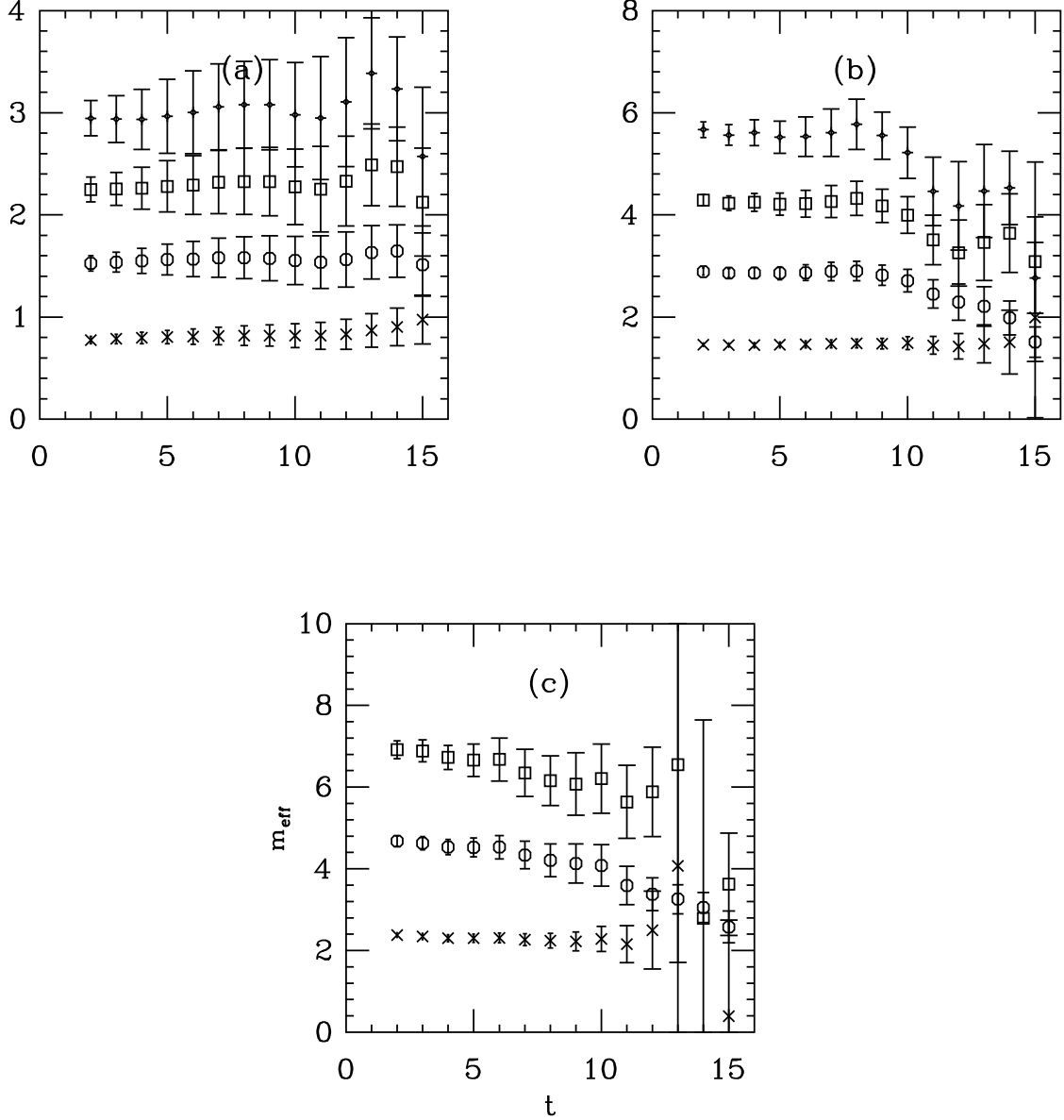


FIG. 6: Effective mass for moments of the highest-spin baryon (higher moments lie higher, so the baryon effective mass is given by crosses, the effective mass of the squared correlator is given by octagons, for the cubed correlator, by squares, and the fancy diamonds are for  $M_4$ ): (a)  $SU(3)$ ,  $\kappa = 0.125$ ; (b)  $SU(5)$ ,  $\kappa = 0.1265$ ; (c)  $SU(7)$ ,  $\kappa = 0.128$ .

be tamed by replacing the average correlator by a truncated cumulant sum,

$$\log \langle C(t) \rangle = \sum_{n=1}^N \frac{\kappa_n}{n!}. \quad (11)$$

Truncation of the sum at some finite  $N$  introduces a systematic error on the mass, but it might be less than the statistical error associated with averaging the original data set. This might give a prediction for  $M$  with a small statistical error. Varying  $N$  and refitting would

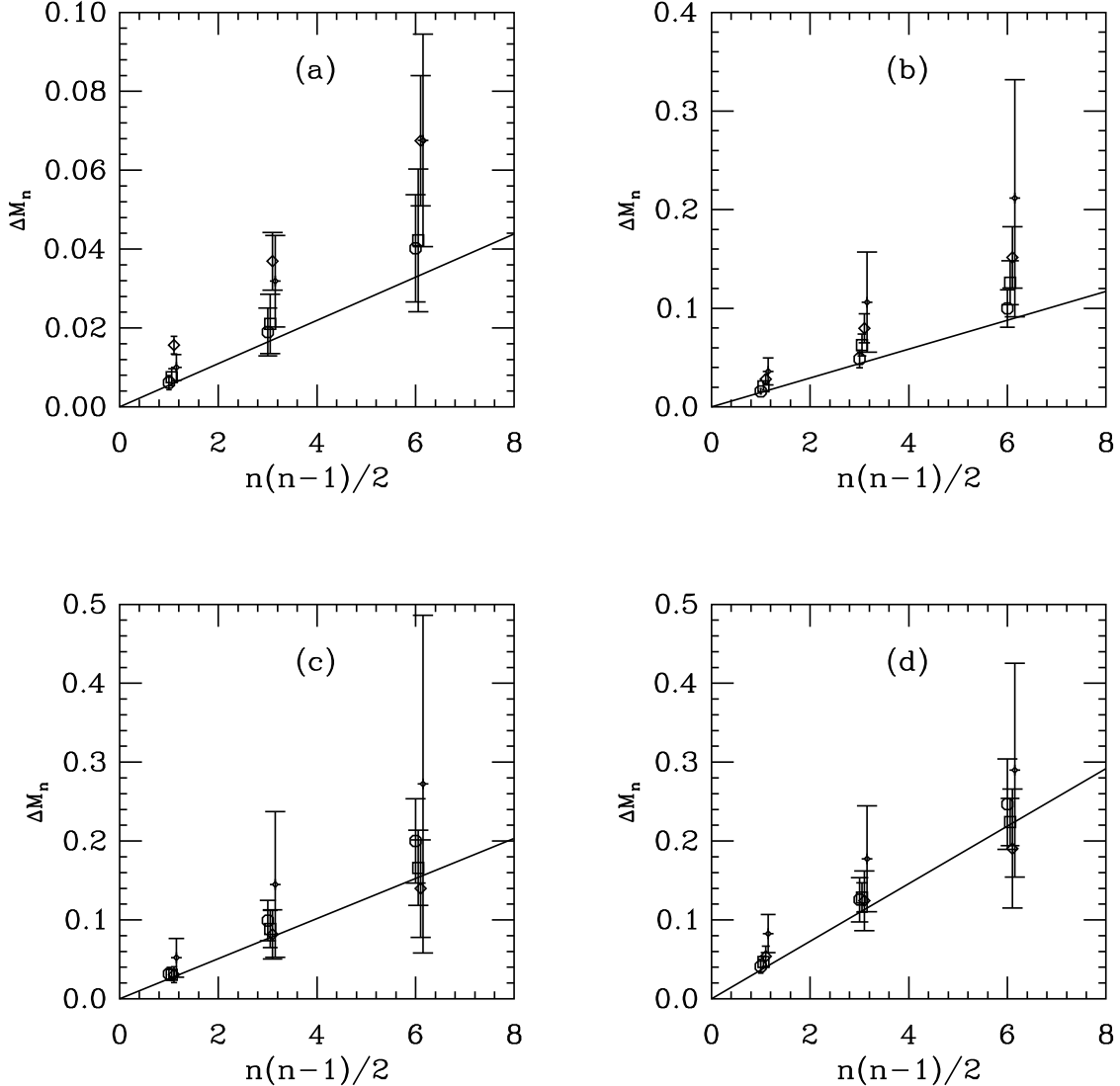


FIG. 7: Effective mass differences  $\Delta M_n = nM_1 - M_n$  hadronic correlators in quenched  $SU(3)$ ,  $\beta = 6.0175$ ,  $\kappa = 0.125$ . Symbols are octagons for  $t = 4$ , squares for  $t = 6$ , diamonds for  $t = 8$  and fancy diamonds for  $t = 10$ . The line is a fit to the slope of  $\kappa_2$  for  $3 \leq t \leq 8$ . (a) pseudoscalar; (b) vector meson; (c) proton; (d) delta.

allow an estimation of the systematic error. Because the cumulants involve all the data, it would be necessary to fold this procedure into a jackknife or bootstrap, and take the uncertainty in the fit parameters from the jackknife or bootstrap average.

An immediate problem doing this is that correlators at different time steps are themselves strongly correlated. Usual fits take this correlation into account in the construction of the correlation matrix for the chi-squared function. Information about time autocorrelations is lost when the cumulant sum is performed time step by time step. If one is doing an effective mass fit with Eq. 8, these correlations do not affect the mean value of  $M$  because the fit has no degrees of freedom. They do affect the uncertainties on the mass and intercept, but presumably a jackknife can handle that. However, serious fits to lattice data are typically

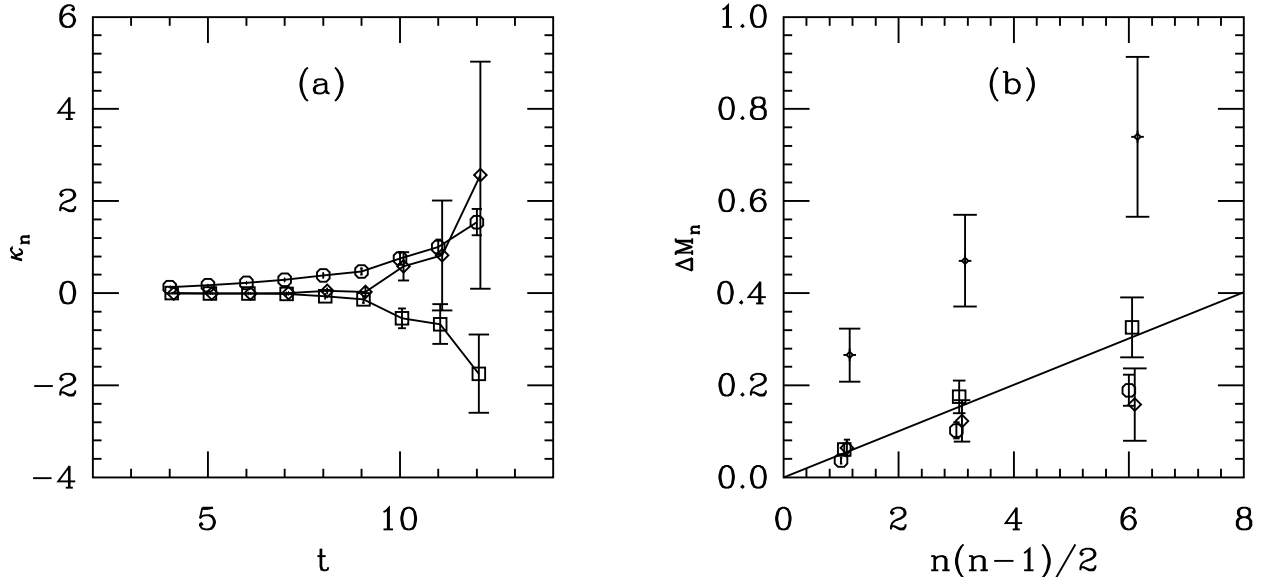


FIG. 8: (a) Cumulants and (b) mass differences for the  $SU(5)$   $J = 5/2$  baryon. In panel (a),  $\kappa_2$ ,  $\kappa_3$  and  $\kappa_4$  are shown by octagons, squares, and diamonds. In panel (b), mass differences at  $t = 4, 6, 8$ , and  $10$  are shown as octagons, squares, diamonds and fancy diamonds. The line is a fit to  $S$ .

“range fits” over many values of  $t$ . Then correlations are important. The author has seen many fits which miss the central values of the individual  $C(t)$ ’s in an asymmetric way, due to the off-diagonal correlations in the data.

For my quenched and dynamical data sets of meson and baryon correlators. I compared conventional effective mass and range fits to fits where  $C(t)$  was replaced by a truncated cumulant sum. Even a truncation ending with  $\kappa_2$  produced fit masses consistent with the usual fits. However, unlike what Refs. [1–7] found, my uncertainties are not improved using the truncated cumulant sum. I show results from a quenched  $SU(3)$  example in Fig. 13. Since the uncertainties are what I want to show, I offset the various orders of the truncated sum by constants. My observations are of course not a blanket statement that the truncated cumulant cannot be used to improve fits, only that I could not do it.

Second, one could take Eq. 9 seriously: the change in the width of the second cumulant measures a mass difference between an  $n$  hadron state in finite volume from  $n$  times the single-hadron state. (This connection was first made in the context of unitary Fermi gases by Nicholson [14].) In QCD, the mass difference gives information on a scattering length  $a$ :

$$\Delta M_n = \frac{4\pi a}{ML^3} \quad (12)$$

for particles in a box of volume  $V$ . Does the data support this? We can test this hypotheses by taking the values of  $S$  from different volumes and just overlaying  $L^3 S$ . Examples were already shown, in Figs. 11 and 12. Sometimes the volume dependence is there.

Curious as it is, this connection cannot be made more precise in QCD. The  $n$ -hadron correlation functions from which my masses are extracted (the moments) are composed of  $n$  distinct color traces. These correlations functions do not project onto a unique isospin, and so the right-hand side of Eq. 12 is – at best – a weighted sum of scattering lengths in

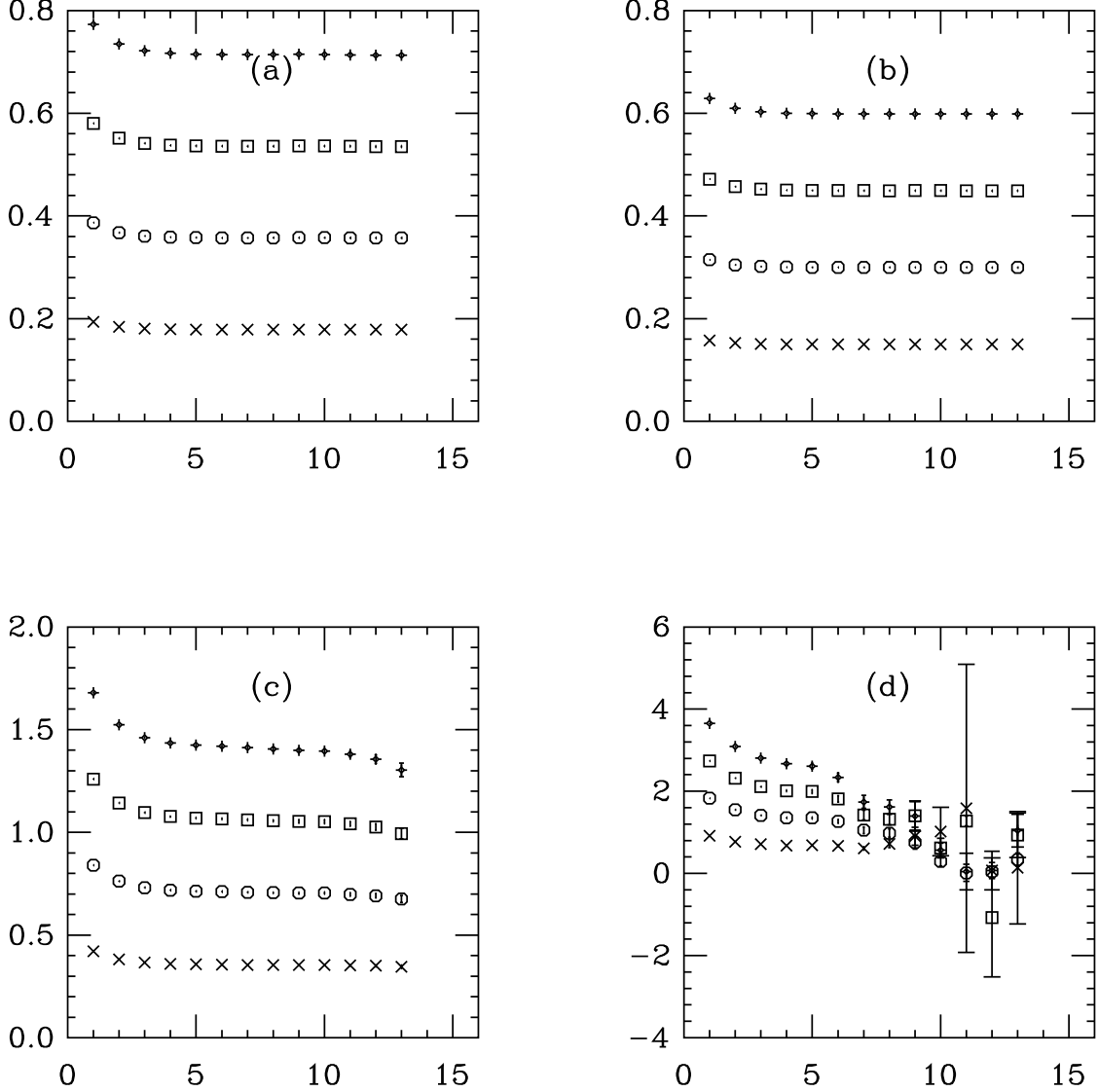


FIG. 9: Effective mass for moments of potentials in quenched  $SU(3)$ ,  $\beta = 6.0175$ . Higher moments lie higher. (a)  $r = 2$  planar loop; (b)  $\vec{r} = (1, 1, 1)$  loop; (c)  $r = 3\sqrt{2}$  loop; (d)  $r = 6\sqrt{2}$  loop.

different isospin channels. And in QCD, three-body interactions have been measured by at least one group [15]. They are not zero.

Since I do not have any crisp conclusions, I will finish with some questions. First, is this behavior really ubiquitous? It would be very interesting to look at distributions of correlation functions for two cases for which I don't have data: One is simulation data from large lattices and small quark masses, where the lightest states in a generic channel are not single-particle states, but multi-body ones. The rho channel when  $m_\rho \gg 2m_\pi$  is an example. Another example would be correlation functions of operators which are highly tuned (say from a variational calculation) to project on a single state. I am also not satisfied with my comparisons of different volumes.

Second, if log-normality is there, why is it there? Since I see it in so many channels, it can't be a consequence of the kind of correlator (baryon versus meson) or system (confining versus

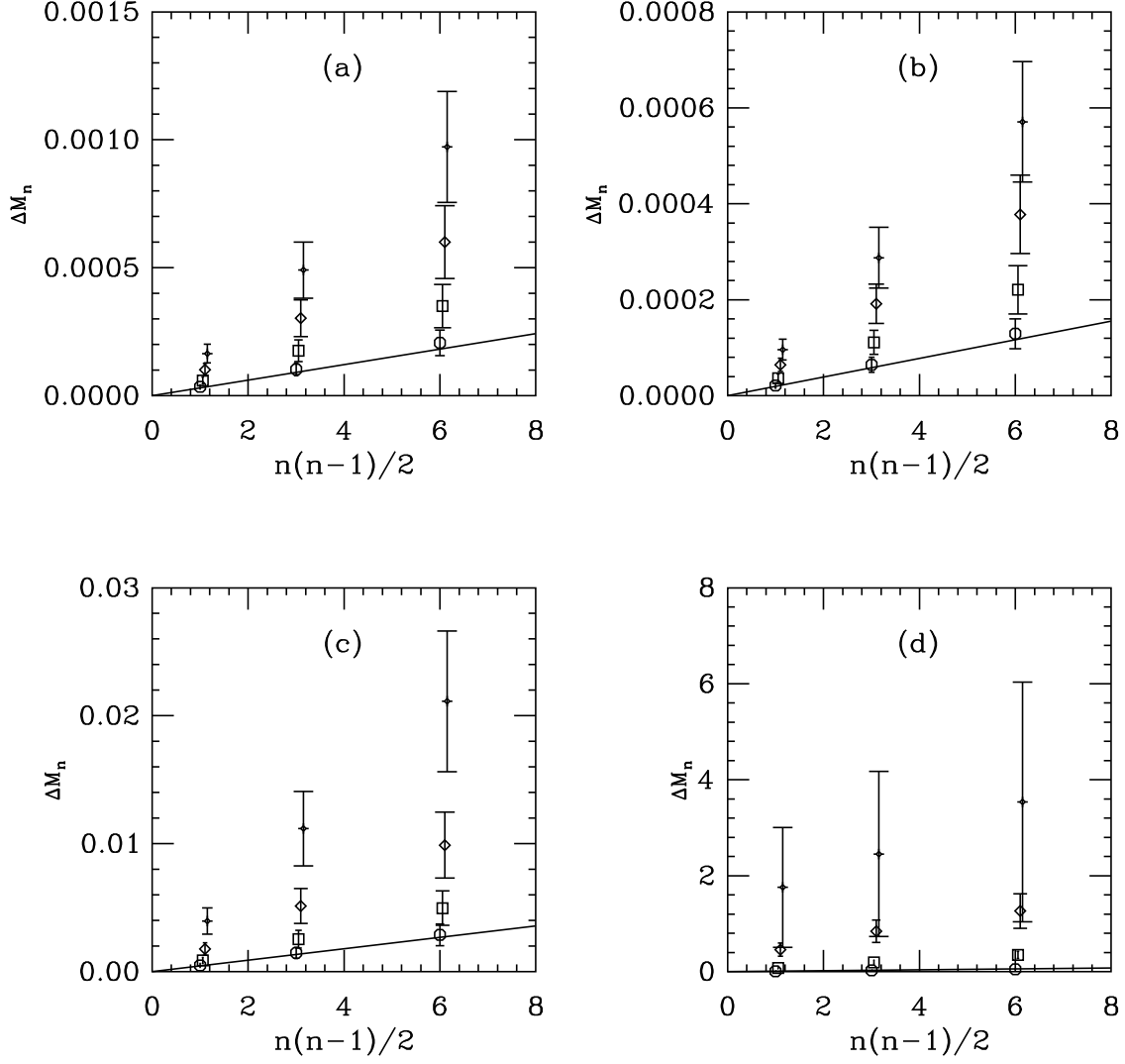


FIG. 10: Effective mass differences  $\Delta M_n = nM_1 - M_n$  from Wilson loops in quenched  $SU(3)$ ,  $\beta = 6.0175$ . Symbols are octagons for  $t = 4$ , squares for  $t = 6$ , diamonds for  $t = 8$  and fancy diamonds for  $t = 10$ . (a)  $r = 2$  planar loop; (b)  $\vec{r} = (1, 1, 1)$  loop; (c)  $r = 3\sqrt{2}$  loop; (d)  $r = 6\sqrt{2}$  loop.

conformal). Log-normal distributions commonly arise when an observable is a product of a set of a set of independent positive random numbers. The variables in a lattice simulation of QCD are matrices, not numbers, and they are not completely random either – the action weights the likelihood of a configuration. One thing that all the correlators I have examined have in common is that they involve products of link matrices, and the number of link matrices involved in a correlator increases with its  $t$  value. This is certainly the case for Wilson loops. Hadronic correlators are built of quark propagators. Quark propagators are themselves sums of products of link variables connecting the source and the sink points of the propagator. Because of the additive property of cumulants, the cumulants of the log of the product of  $\tau$  random variables are equal to  $\tau$  times the cumulant of the individual distributions. This certainly has the flavor of the linear increase in  $\kappa_2(t)$  observed in the

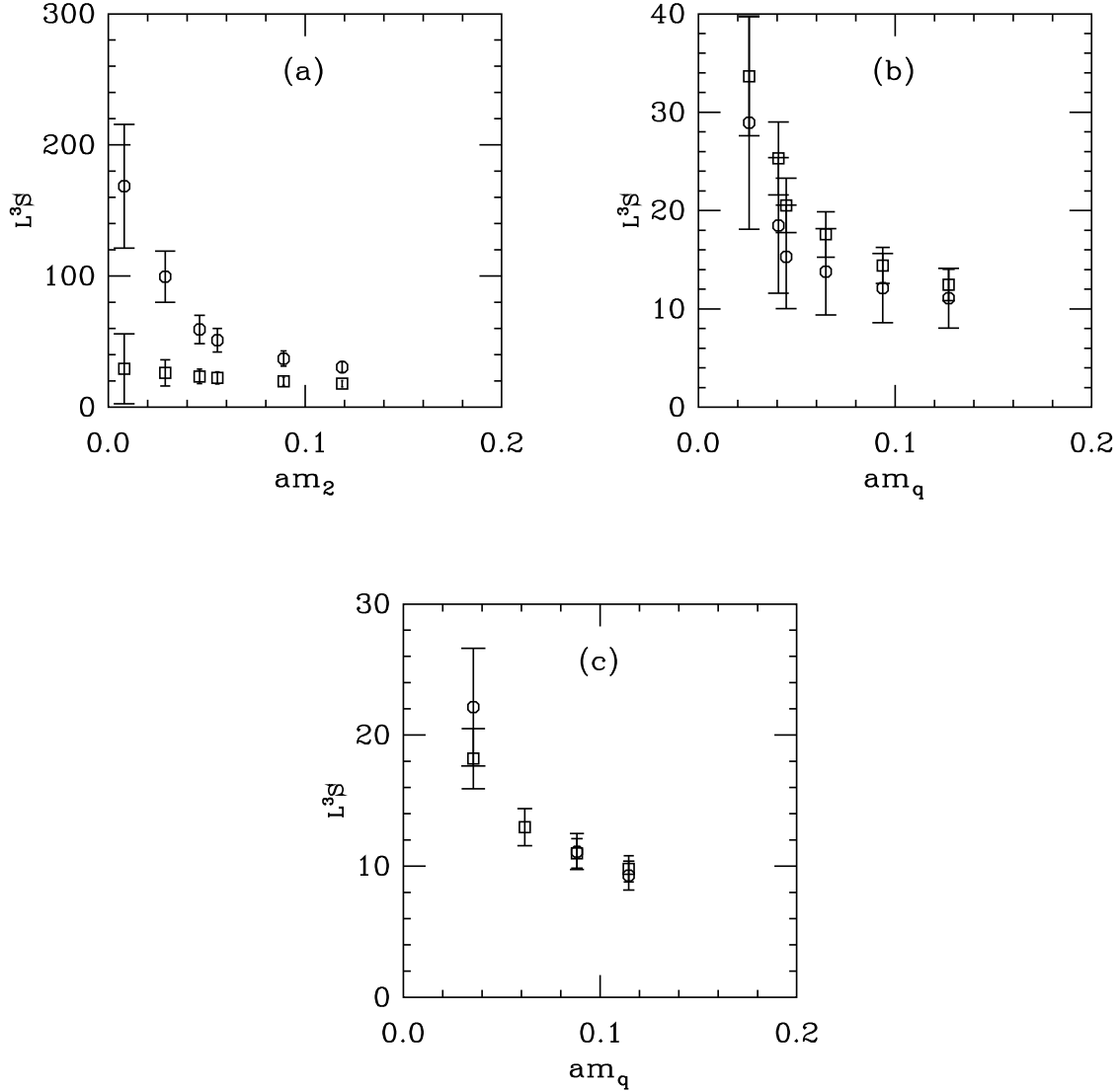


FIG. 11: Parameter  $S$  from the slope of  $\kappa_2$  with  $t$ , from Eq. 7 for pseudoscalar correlators from quenched simulations. Squares  $16^3$  volume; octagons,  $12^3$  volume. (a)  $SU(3)$  (b)  $SU(5)$  (c)  $SU(7)$ . The  $x$  axis is the AWI quark mass and all three data sets are matched in lattice spacing.

data.

And finally, can log-normality be used to do anything quantitative? So far, I have not been able to use it to improve mass determinations along the lines of [1–7].

As I said at the start, I am not sure whether approximate log-normality in lattice correlator data is useful for anything. However, I have to say: I have been looking at lattice data for a long time, and it is quite curious to observe something new and (apparently) generic in it.

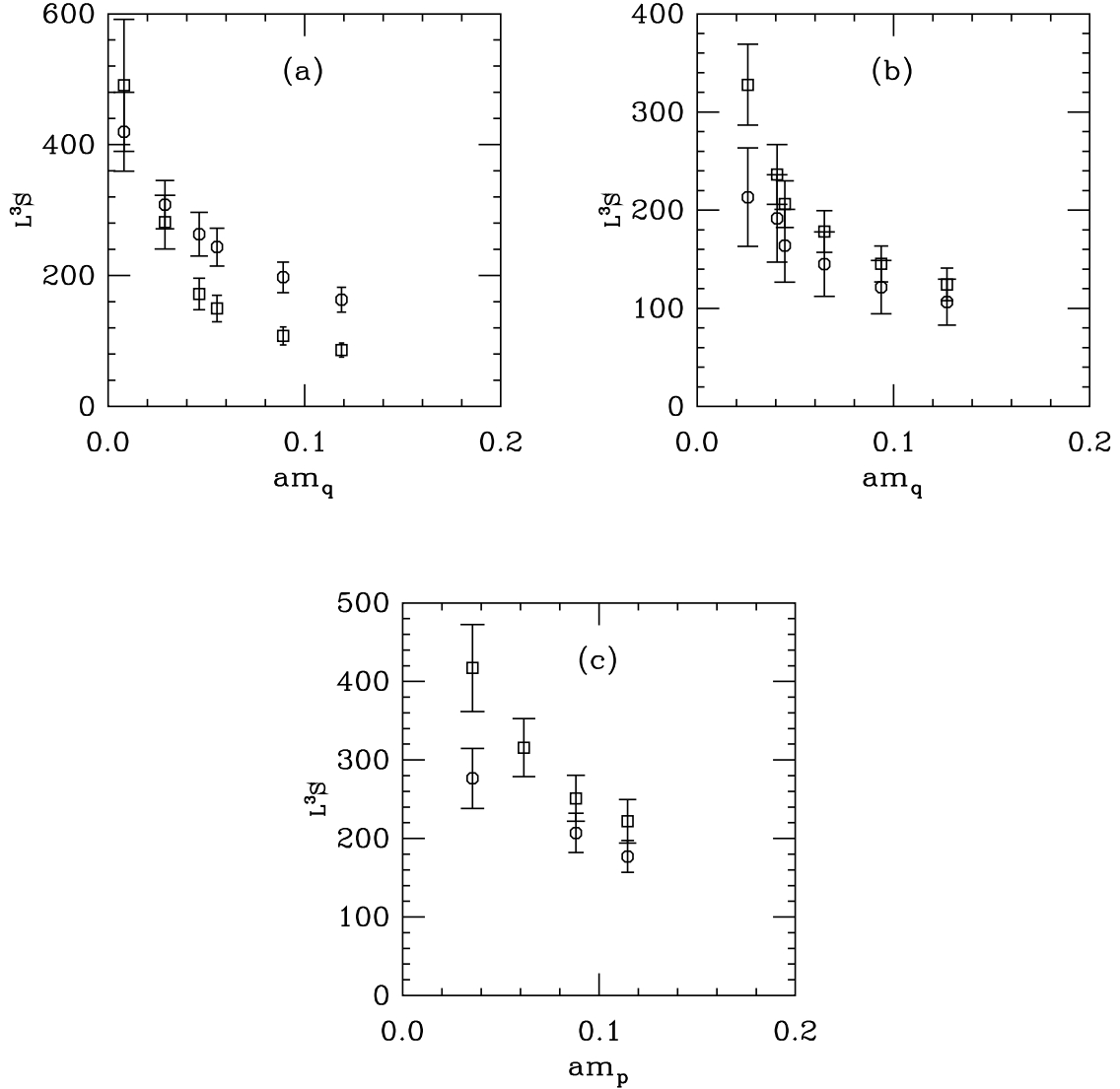


FIG. 12: Parameter  $S$  from the slope of  $\kappa_2$  with  $t$ , from Eq. 7, scaled by the spatial simulation volume, for the highest-spin baryon from quenched simulations. Squares  $16^3$  volume; octagons,  $12^3$  volume. (a)  $SU(3)$  (b)  $SU(5)$  (c)  $SU(7)$ . The  $x$  axis is the AWI quark mass and all three data sets are matched in lattice spacing.

### Acknowledgments

I would like to thank M. G. Endres, D. B. Kaplan, J. -W. Lee and A. N. Nicholson for much correspondence and conversation. Their Ref. [1] directly inspired this investigation. This work was supported by the U. S. Department of Energy.

---

[1] M. G. Endres, D. B. Kaplan, J. -W. Lee and A. N. Nicholson, arXiv:1112.4023 [hep-lat].

[2] J. -W. Lee, M. G. Endres, D. B. Kaplan and A. N. Nicholson, PoS LATTICE **2011**, 203

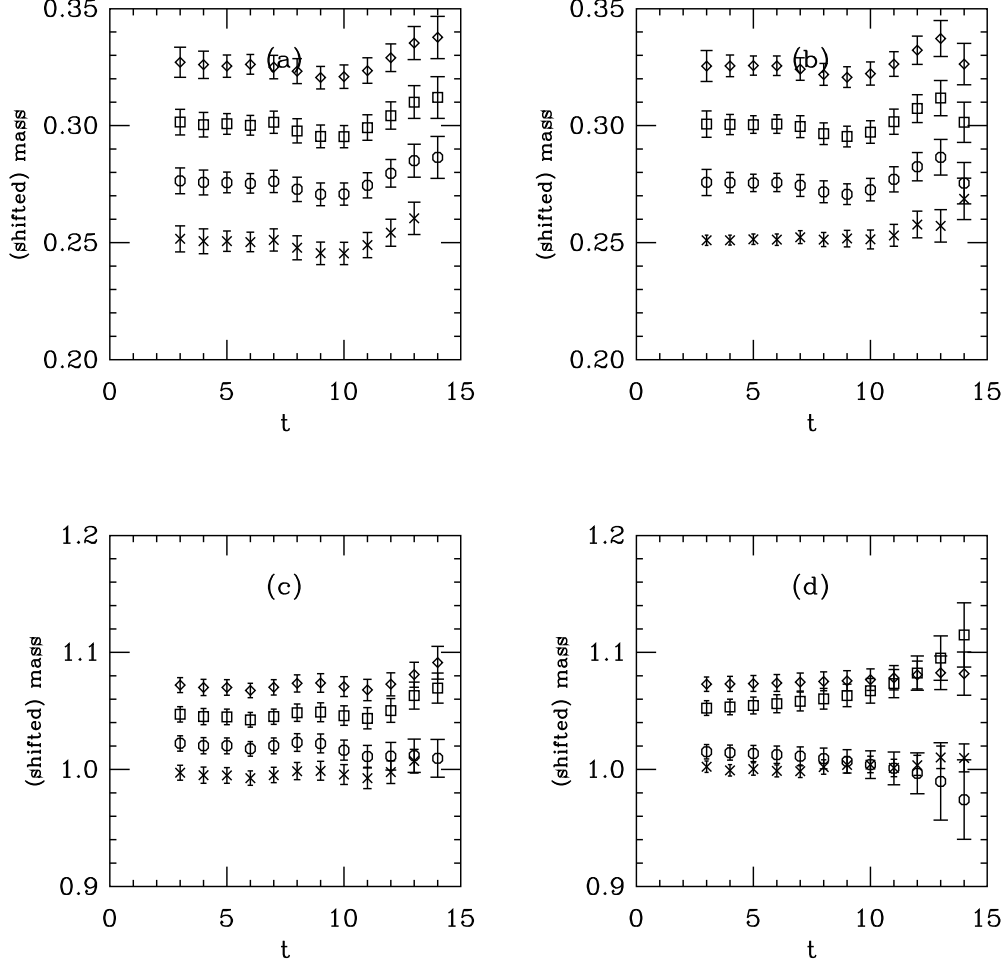


FIG. 13: Conventional and truncated cumulant fits to data, quenched  $SU(3)$ ,  $\beta = 6.0175$ . Crosses show the conventional fit result. Octagons, squares and diamonds truncate the sum at  $n = 2, 3, 4$ , and the fit values are shifted vertically by multiples of 0.025. Panels (a) and (b) show effective mass and range fits for the pseudoscalar, at  $\kappa = 0.126$ , and panels (c) and (d), for the delta, at  $\kappa = 0.123$ .

- (2011) [arXiv:1111.3793 [hep-lat]].
- [3] M. G. Endres, D. B. Kaplan, J. -W. Lee and A. N. Nicholson, Phys. Rev. A **84**, 043644 (2011) [arXiv:1106.5725 [hep-lat]].
- [4] M. G. Endres, D. B. Kaplan, J. -W. Lee and A. N. Nicholson, arXiv:1106.0073 [hep-lat].
- [5] M. G. Endres, D. B. Kaplan, J. -W. Lee and A. N. Nicholson, PoS LATTICE **2010**, 182 (2010) [arXiv:1011.3089 [hep-lat]].
- [6] A. N. Nicholson, M. G. Endres, D. B. Kaplan and J. -W. Lee, PoS LATTICE **2010**, 206 (2010) [arXiv:1011.2804 [hep-lat]].
- [7] J. -W. Lee, M. G. Endres, D. B. Kaplan and A. N. Nicholson, PoS LATTICE **2010**, 197 (2010) [arXiv:1011.3026 [hep-lat]].
- [8] The data was provided by W. Detmold using results from the NPLQCD collaboration.
- [9] A. Hasenfratz and F. Knechtli, Phys. Rev. D **64**, 034504 (2001) [arXiv:hep-lat/0103029].
- [10] A. Hasenfratz, R. Hoffmann and S. Schaefer, JHEP **0705**, 029 (2007) [arXiv:hep-lat/0702028].



- [11] G. P. Lepage, “The Analysis Of Algorithms For Lattice Field Theory,” invited lectures at the 1989 TASI summer school, Boulder CO, June 4-30, 1989. CLNS-89-971.
- [12] M. Luscher, Commun. Math. Phys. **104**, 177 (1986).; Commun. Math. Phys. **105**, 153 (1986).
- [13] This remark is credited to M. Savage by D. B. Kaplan in [1].
- [14] A. N. Nicholson, arXiv:1202.4402 [cond-mat.quant-gas].
- [15] W. Detmold, M. J. Savage, A. Torok, S. R. Beane, T. C. Luu, K. Orginos and A. Parreno, Phys. Rev. D **78**, 014507 (2008) [arXiv:0803.2728 [hep-lat]].